Published in final edited form as:
Arterioscler Thromb Vasc Biol. 2013 November ; 33(11): 2566–2576. doi:10.1161/ATVBAHA.113.301903.

Novel role of CD47 in rat microvascular endothelium: signaling and regulation of T cell transendothelial migration

Roberta Martinelli[1,2,3], **Gail Newton**[1], **Christopher V. Carman**[2], **John Greenwood**[3], and **Francis W. Luscinskas**[1]

[1]Center for Excellence in Vascular Biology, Department of Pathology, Brigham and Women's Hospital and Harvard Medical School, Boston, MA 02115

[2]Center for Vascular Biology Research, Department of Medicine, Beth Israel Deaconess Medical Center and Harvard Medical School, Boston, MA 02215

[3]Department of Cell Biology, Institute of Ophthalmology, UCL, London UK

Abstract

Objective—Although endothelial CD47, a member of the Ig superfamily, has been implicated in leukocyte diapedesis, its capacity for intracellular signaling and physical localization during this process has not been addressed in detail. This study examined endothelial CD47 spatial-temporal behaviour and signaling pathways involved in regulating T cell transendothelial migration (TEM).

Approach and Results—By biochemical methods, transmigration assays and live cell microscopy techniques, we show that endothelial CD47 engagement results in intracellular calcium mobilization, increased permeability and activation of src and AKT1/PI3K in brain microvascular endothelial cells. These signaling pathways converge to induce cytoskeleton remodeling and Vascular Endothelial Cadherin (VEC) phosphorylation, which are necessary steps during T cell TEM. Additionally, during T cell migration, transmigratory cups and podoprints enriched in CD47 appear on the surface of the endothelium, indicating that the spatial distribution of CD47 changes following its engagement. Consistent with previous findings for ICAM1, blockade of CD47 results in decreased T cell transmigration across microvascular endothelium. The overlapping effect of ICAM1 and CD47 suggests their involvement at different steps in the diapedesis process.

Conclusions—These data reveal a novel role for CD47 mediated signaling in the control of the molecular network governing endothelial dependent T cell diapedesis.

Keywords

CD47; endothelium; transmigration; leukocytes; signaling

Correspondence: Francis W. Luscinskas, Department of Pathology, Brigham and Women's Hospital, 77 Avenue Louis Pasteur, Boston, MA 02115, Fax: 617-525-4333; Tel: 617-525-4307. fluscinskas@rics.bwh.harvard.edu.

Contributions: R.M. designed and performed research, analyzed data, performed statistical analysis, co-wrote manuscript; G.N. performed research and collected and analyzed data; C.V.C. designed and performed research, analyzed and interpreted data; J.G. contributed vital new reagents; F.W.L. designed research, interpreted data, co-wrote manuscript.

Conflict of interest disclosure:
The authors declare no competing financial interests.

Introduction

The endothelial cell (EC) monolayer plays an active role in the recruitment of leukocytes from the bloodstream into tissues both during immune cell surveillance and inflammatory responses. Examples of its pro-active functions are endothelial adhesive platforms (EAPs), tetraspanin enriched domains that facilitate leukocyte adhesion (reviewed in[1]), ICAM1 clustering accompanying neutrophil diapedesis and the formation of docking structures surrounding the transmigrating leukocyte through the extension of "endothelial microvilli" [2,3] forming a cup-like structure [4]. Additionally, signaling events occurring within ECs are critical for the control of the sequential multistep cascade leading to leukocyte transendothelial migration (TEM)[5,6]. Different adhesion molecules have been shown to transmit important outside-in signals[5,7,8] and interference with these pathways impaired lymphocyte TEM without affecting adhesion.

CD47, or Integrin Associated Protein, is a member of the Ig superfamily. CD47 interacts "in trans" with thrombospondin-1 (TSP-1) and two members of the signal regulatory protein family (SIRP), SIRPα and SIRPγ, and "in cis" with αvβ3 and α2β1 integrins[9]. In vivo studies indicate that CD47 is involved in neutrophil migration in a murine peritonitis model[10], a lipopolysaccharide-induced acute lung injury and bacterial pneumonia model[11], a trinitrobenzenesulfonic acid-induced colitis model[12], hapten-stimulated dermal inflammation[13], and in a dermal air pouch model[14]. Additionally, in rat brain microvascular ECs the interaction of CD47 with its monocyte-expressed ligand SIRPα was shown to contribute to the final step of monocyte trafficking[15]. In vitro, CD47 plays a role in neutrophil[16] and monocyte migration across epithelial monolayers[17]. Recently, it has been shown that endothelial CD47 interaction with SIRPγ is required for T cell TEM in human umbilical vein EC (HUVEC)[18]. Although most CD47-mediated cellular responses probably involve the activation of integrins, its ability to induce outside-in signaling in brain microvascular endothelium has not been explored in detail during leukocyte recruitment. The purpose of this study was to investigate whether endothelial CD47 is able to induce endothelial signaling and to characterize CD47 spatiotemporal dynamics during T cell TEM in an in vitro model of rat brain endothelium.

Results

Rat CD47 cell surface expression and localization in rat brain microvascular endothelial cells

Rat CD47 is characterized by a single extracellular IgV domain, five transmembrane spanning domains and a short alternatively spliced intracellular cytoplasmic tail. We first assessed the cell surface expression of CD47 both in primary rat brain microvascular EC (MVEC) and in the rat brain microvascular endothelial cell line GPNT by flow cytometry. CD47 was expressed at similar levels under noninflammatory conditions in both EC and did not change significantly with TNF-α, IFN-γ or a combination of the two for 4h or 24h (Fig 1A). Consistent with a previous report[15], these data indicate that CD47 is constitutively expressed in rat brain microvasculature. The staining pattern of CD47 in both resting and TNF-α treated endothelium (Fig 1B) showed uniform apical expression and enrichment at cell-cell junctions as previously reported in HUVEC[18] and murine lung EC[19]. Vascular

Endothelial Cadherin (VEC) staining is shown for comparison. Flow cytometry and immunofluorescence experiments performed under permeabilizing conditions showed a lack of significant intracellular pools of CD47 (data not shown).

CD47 engagement results in receptor clustering and actin rearrangement in MVECs

CD47 redistribution on the surface of brain MVEC was investigated following antibody crosslinking, which mimics lymphocyte adhesive interactions[20–22]. Five min after crosslinking CD47 was recruited into surface clusters (Fig 2A as emphasized in x–y intensity plot beneath panels a–c and data not shown). At the later time point of 60 min, an increase in surface cluster size was observed (Fig 2B). Although CD47 intracellular tail lacks any recognized signaling motif, we hypothesized that CD47 engagement might elicit signaling events that couple to cytoskeletal rearrangement. Indeed, actin rearrangement could be observed following CD47 crosslinking. However, contrary to results in confluent HUVEC monolayers[18], CD47 engagement in GPNT cells induced formation of cortical bundles of actin fibers rather than stress fibers (Fig 2A and C). Interestingly, 60 min post CD47 crosslinking, VEC staining appears less continuous and more jagged than the control condition (Fig 2C, bottom panel, arrows).

There is growing evidence that adhesion molecules are recruited to specialized microdomains of the plasma membrane enriched in cholesterol, sphingomyelins and glycosphingolipids (lipid rafts), and that this localization to rafts regulates intracellular signaling and leukocyte transendothelial migration. To test whether CD47 is associated with lipid rafts, the endothelial cell monolayer was pre-treated with filipin to sequester cholesterol and thus disrupt rafts [23]. Upon disruption of the lipid microdomains, CD47 showed less localization to cell-cell junction, and crosslinking of CD47 for 60 min failed to induce CD47 clustering or actin rearrangements (Fig 2D). A control of filipin treatment of EC alone is shown (Fig 2D).

Engagement of endothelial CD47 induces calcium mobilization in microvascular endothelium

Addition of neutrophils on EC monolayers has been reported to induce calcium mobilization from ECs [24,25]. Indeed addition of rat T cells on GPNTs monolayers induced calcium mobilization (Fig 3A). To dissect the possible role of CD47 in the intracellular calcium mobilization, we performed CD47 antibody cross-linking experiments. Using GPNT monolayers, we show that addition of anti-CD47 monoclonal antibody (mAb) alone resulted in a modest and transient elevation of intracellular calcium (Fig 3B). However, CD47-crosslinking by goat-anti-mouse (GAM) secondary antibody triggered a rapid (within 1 min) and a more robust elevation in intracellular calcium that exhibited persistent oscillatory behavior. As a comparison, the mobilization of intracellular calcium was investigated in GPNT cells following ICAM1 antibody crosslinking. The addition of the primary antibody alone elicited robust calcium release, as previously reported[22] (Fig 3C), whereas subsequent crosslinking with GAM induced a second phase of calcium oscillations of lesser intensity. Similar results were observed in primary rat brain MVEC (data not shown). As expected, pre-treatment of the endothelium with the cell permeant calcium chelator BAPTA-2AM ablated intracellular calcium fluxes upon CD47 engagement (Fig 3D). Pre-treatment of the

EC with the src inhibitor PP2 did not affect the initial calcium flux induced by crosslinking, but completely blocked the subsequent oscillatory phase (Fig 3E). Crosslinking of Major histocompatibility complex Class I (MHC-I), a molecule not involved in leukocyte recruitment, or with of an irrelevant isotype-matched mAb (mouse IgG1) had no effect (Fig 3F and 3G). These data indicate that crosslinking and clustering of CD47 triggers mobilization of intracellular calcium in MVEC that involves src family kinases.

Engagement of endothelial CD47 induces intracellular src and AKT signaling in microvascular endothelium

Because src and AKT proteins were linked to CD47 signaling[26], we investigated their activation in GPNT. Following 5 min of CD47 crosslinking, src kinases became phosphorylated (activated p-src) and their activation was maintained for 60 min (Fig 3H). Phospho-AKT (p-AKT) was also induced by CD47 engagement, but occurred later at 30 min and more transiently (Fig 3I). These results were confirmed in freshly isolated primary brain MVEC (Fig 3J and 3K).

Dissecting the CD47 intracellular signaling pathways

We next performed experiments to understand the spatio-temporal sequence of activation events initiated by CD47 crosslinking. Pretreatment of GPNT cells with Pertussis toxin (PTX) significantly reduced CD47-mediated phosphorylation of AKT and src, indicating a role for Gi proteins upstream of these molecules (Fig 4A, panels a – c). Similarly, the src inhibitor PP2 abolished CD47 induced signaling responses in src and AKT, suggesting src is more proximal in the signaling pathway. The PI3K inhibitor LY294002 induced a high basal level of phospho-src (p-src) and reduced the response to CD47 crosslinking. Additionally, LY294002 treatment inhibited CD47-mediated AKT phosphorylation that reached significance only at 60 min. Finally, the inhibitor C3 transferase was used to assess the dependence of the CD47 pathway on RhoA/B/C GTPases. Pretreatment of the endothelium with C3 transferase induces a higher basal level of p-src and had no effect on CD47 mediated phosphorylation of src or AKT as compared to non-crosslinked control conditions (Fig 4A).

Based on our initial findings that CD47 antibody crosslinking resulted in receptor clustering on the surface of the endothelium, and that clustering was coupled to actin rearrangements, we investigated whether the same pharmacological inhibitors used above altered CD47 clustering. Rho inhibition by C3 transferase or src inhibition (PP2) abolished CD47 mediated surface clustering following its crosslinking (Fig 4B). Pretreatment of the endothelium with PTX, however, did not affect receptor clustering at 60 min while LY29004 had lesser effect on the size of CD47 surface clusters (Fig 4B, panels c and f). That downstream events such as src and Akt activation still occur in C3 treated GPNT despite its inhibition of CD47 clustering was unexpected and at present the mechanisms remains unknown.

Downstream effect of CD47 engagement include VEC phosphorylation, modification of permeability and lymphocyte migration

Because ICAM1 regulates leukocyte migration through a pathway involving phosphorylation of VEC [21,27,28], we asked whether CD47 engagement induced phosphorylation of VEC in GPNT cells. Crosslinking of CD47 led to a 1.5 fold-increase in the levels of phosphorylation of VEC as early 5 min and was maintained up to 60 min as assessed by phosphotyrosine specific polyclonal Ab 4G10. Thrombin stimulation induced a comparable level of VEC phosphorylation (Fig 5A). We next evaluated if inhibitors affected phosphorylation of VEC at Tyr658 or Tyr731 after 30 min of CD47 crosslinking using phosphospecific polyclonal Abs. As shown in Fig 5B, an increase in phosphorylation of Tyr731 was detected upon CD47 crosslinking whereas no significant change occurred in Tyr658. Each treatment inhibited the increase in phosphorylation of Tyr731 and PP2 also reduced basal level of Tyr731.

We next investigated whether CD47 engagement altered EC permeability to dextran-FITC (70kDa), using thrombin stimulation as a positive control. As expected, addition of thrombin resulted in disruption of barrier function as indicated by the increase in the measured fluorescence. A comparable increase in the dextran-FITC fluorescence was observed following CD47 crosslinking, while ICAM1 crosslinking had a smaller effect (Fig 5C).

In the next set of studies we observed that mAb blockade of CD47 or ICAM1 significantly decreased transmigration compared to isotype IgG1 control mAb (Fig 5D). Blockade of CD47 did not affect lymphocyte adhesion, whereas blocking ICAM1 reduced adhesion. The combination of ICAM-1 and CD47 mAb blocking was not additive (data not shown). Collectively, the results from Figures 4 and 5 suggest a model for CD47-induced signaling in microvascular brain EC monolayers that involves mobilization of intracellular calcium, src, AKT and RhoGTPase activation that lead to VEC phosphorylation, actin rearrangement and reduced barrier function (Fig 5E).

Endothelial CD47 is redistributed to the site of migration: evidence of podoprints and transcellular cup enriched in CD47

Given our established role for CD47 engagement in TEM, we examined CD47 cell surface distribution dynamics during T cell TEM. Initially we conducted live-cell imaging of T cells migrating over human lung MVECs transfected to express a general plasma membrane marker (Mem-DsRed) and human CD47-GFP. The CD47-GFP functionality was demonstrated by its ability to mobilize intracellular calcium in OV-10 cells upon crosslinking (Figure S1). These studies revealed dynamic formation of micron-scale fluorescent Mem-DsRed rings beneath apical migrating T cells (i.e., podo-prints, a read-out for T cell formation of podosome-like protrusions[29]). Strikingly, these regions of intimate T cell-endothelial contact were strongly enriched in CD47, as measured by line-scan analysis (Fig 6A and panels g–h). As a control, we performed studies with CD40-GFP, a molecule in endothelium that is not involved in TEM. As expected, CD40 did not show any enrichment at the site of podosomes (data not shown). In the second approach, MBP activated rat T cells were incubated with GPNT monolayers for 15 min, washed, fixed, stained and analyzed for TEM by confocal microscopy. Confocal scans through sequential planes in the z-axis

showed finger-like endothelial protrusions enriched in CD47 partially enveloped the migrating T cell (Fig 6B). Orthogonal images further emphasized the formation of a transmigratory cup enriched in CD47 (Fig 6B; video S1). Quantification of transmigrating T cells showed that in 67% of events, CD47 is associated with the transmigratory cup (Fig 6B). Live-cell microscopy experiments conducted on human CD47-GFP transfected human lung MVECs confirmed the strong enrichment of CD47 around transmigrating T cells (Fig 6C and video S2). Because ICAM1 and VCAM1 become enriched at the transmigratory cup, we investigated whether endothelial CD47 co-localized with these molecules. Because CD47 is also expressed on T cells, to distinguish the endothelial CD47 contribution, 10 μm diameter polyester beads to imitate T cells were coated with an anti-ICAM1 mAb and incubated with EC for 20 minutes. Co-localization was detected through Pearson's analysis and showed that CD47 co-localizes with both ICAM1 and VCAM1 at sites of T cell transmigration (Figure 6D; graph b (r= 0.68±0.035 and 0.56±0.087, respectively, p = 0.043).

Discussion

Our current findings demonstrate that in brain microvascular endothelium, CD47 is enriched at cell-cell junctions and readily clusters upon antibody-induced crosslinking. We, therefore, envision that CD47 redistribution at the apical endothelial surface is an important step for signal transduction and T cell transmigration. Consistent with this idea, alteration in the membrane fluidity by cholesterol extraction with filipin prevents CD47 clustering and results in loss of actin rearrangement in brain MVEC (Fig 2). The effect by filipin suggests that CD47 is organized in specific lipid plasma membrane domains. Indeed, organization of CD47 into lipid rafts has been previously shown to be necessary for actin polymerization and Protein Kinase C translocation in T cells[30]. In the context of leukocyte migration, organization of ICAM1, VCAM1 and the tetraspanins CD9 and CD151 in preformed lipid-enriched membrane microdomains has been shown to be part of a "signaling machinery" that regulates leukocyte TEM[1]. Here we demonstrate that CD47 is also enriched in endothelial microvilli-like projections and colocalizes with ICAM1 and VCAM1 and clusters around migrating lymphocytes. ICAM1 and VCAM1 associate during leukocyte migration in 'docking structures', 'ring-like structures' or 'transmigratory cups' that facilitate transmigration[2–4,20]. We suggest, therefore, that CD47 is present at the plasma membrane in a molecular complex with ICAM1, VCAM1 and tetraspanins, and possibly integrins, which together regulate leukocyte TEM[1]. Our studies do not distinguish whether CD47 plays an active role in the formation of these structures or accumulates because it is physically associated with other molecules that function in TEM. Future studies are necessary to address this question. We have also shown that beneath T cells migrating on the apical MVEC surface, endothelial CD47 redistributes and becomes enriched at 'podo-print' invaginations that facilitate junctional and non-junctional TEM[29].

We show that despite its short intracellular domains that lack known signaling modules, endothelial CD47 engagement results in intracellular calcium mobilization that exhibits oscillatory behavior, and downstream activation of src and AKT/PI3K in rat brain microvascular EC. Our data also provide evidence that CD47 crosslinking induces an increase in VEC phosphorylation in brain MVEC, and in particular, a modest but significant increase at residue Tyr 731. Additionally our results suggest that other VEC tyrosine

residues are involved, but phosphospecific Ab reagents are not currently available to test this idea. As previously demonstrated in rat brain MVEC, T cell engagement of ICAM1 results in phosphorylation of VEC in a calcium, src and eNOS dependent manner[22]. Tyrosine to phenylalanine substitutions in the intracellular domain of VEC at positions 645, 731 or 733 affect lymphocyte migration in a dominant manner in the same system[21]. Other studies using cultured human endothelium have reported that engagement of ICAM-1 and CD47 triggers phosphorylation of VEC Tyr658 and Tyr731, and that overexpression of VEC mutants Y731F and Y658F blocks leukocyte TEM. Thus phosphorylation of VEC plays an important role in leukocyte TEM [14, 21,26,27, 28,30,31]. Signaling pathways that lead to VEC phosphorylation probably function as a common mechanism through which adhesion molecules control leukocyte transmigration. Our experiments showing that CD47-induced VEC phosphorylation depends on Gi, src and AKT (Figs 4 and 5) corroborate this conclusion. We speculate that CD47 crosslinking induces calcium mobilization and Gi-coupled signals that contribute to VEC tyrosine phosphorylation, although further experiments are necessary to pinpoint their precise role(s). Importantly, all agents that blocked CD47-mediated VEC phosphorylation, with the exception of LY294002, have been previously shown to significantly reduce lymphocyte transmigration in a similar experimental system[32,33]. It is also likely that CD47 engages additional signaling pathways based on previous reports in other cell types. CD47 was first identified by its coimmunoprecipitation with αvβ3 integrin in platelets and was called Integrin Associated Protein[9]. Several reports demonstrated that CD47 physically interacts with and regulates certain integrins and acts directly or indirectly as a signal transduction molecule[34]. Whether CD47 signals directly or interacts with EC integrins during leukocyte transmigration or regulating vessel permeability requires further study.

We note that while mAb blocking ICAM1 results in reduced adhesion and transmigration of T cells (Fig 5 and [35]), mAb blockade of CD47 reduces T cell transmigration without affecting adhesion. Interestingly, blockade of both CD47 and ICAM1 during TEM was not additive. These results suggest that in this system CD47 and ICAM1 function in different but complementary steps in the leukocyte trafficking cascade. Similar effects were observed for CD47 in transmigration of monocytes through brain endothelial cells, and thus provide a broader context for this idea[15].

The relationship between leukocyte influx and increased vessel permeability has been a topic of investigation for decades and remains controversial. Recent studies have reported that engagement of ICAM1 increased microvessel permeability in the TNF-α-activated cremaster muscle model[36]. Consistent with this observation, engagement of either CD47 or ICAM1 led to increased EC monolayer permeability. The presence of jagged VEC staining observed at the same time point that corresponds to increased permeability (Fig 2C and 5B), further suggests a role for CD47 in the regulation of vascular permeability. Future in vivo studies are necessary to evaluate the role of CD47 in microvessel permeability.

In conclusion, our studies show that the intracellular signaling pathways downstream of CD47 in the endothelium contribute to the regulation of endothelial monolayer barrier function and of T cell transendothelial migration across brain microvascular EC monolayers in vitro.

Materials and Methods

Endothelial cells

The immortalized Lewis rat brain microvascular endothelial cell (EC) line GPNT and primary cultures of cerebral ECs prepared from 5–7-wk-old Lewis rats were grown as previously described[1]. Primary rat ECs were seeded on collagen IV and fibronectin-coated plates and maintained in EGM-2 MV (Lonza, Hopkinton, MA). All rats used in our studies were used in accordance with the guidelines of the Committee of Animal Research at the Harvard Medical School and the NIH Animal research guidelines. Human lung microvascular endothelial cells (HLMVEC) were purchased from Lonza and maintained in EBM-2 with full supplements (Lonza).

Plasmids and transfections

Human CD40-GFP was obtained from Matthew Krummel (University of California, San Francisco). Membrane monomeric DsRed was purchased from Clontech (Mountain View, CA). Human CD47 full length was cloned into pEGFP-N1 using standard techniques as previously described[2]. To assess the functional activity of the CD47-GFP construct, intracellular calcium mobilization experiments were performed in the OV-10 cell line lacking CD47 (kindly provided by Professor William Frazier, Washington University, St. Louis MO), following transfection with CD47-GPF and CD47 cross-linking (Figure 1S). Subsequently, GPNT cells or primary human lung microvascular endothelial cells (HLMVEC) were nucleofected using 10 μg plasmid per 0.5×10^6 cells/transfection according to the manufacturer's instructions (Amaxa, Lonza).

Flow cytometry

Confluent rat brain and GPNT cell monolayers were incubated in culture medium alone or medium with cytokines as described. CD47 was detected with OX101 mAb (clone sc-53050, Santa Cruz, Dallas, TX) followed by incubation with a FITC-labeled secondary mAb and analyzed on a FACScan instrument (BD Biosciences, Mountain View, CA).

CD47 crosslinking and inhibitors treatment

Confluent serum starved, TNF-α stimulated GPNT cells were either left untreated ("-") or crosslinked by addition of anti-CD47 mAb (10 μg/ml for 30 min) followed by goat-anti mouse Ab (GAM, 10 μg/ml) addition for the indicated times. Where indicated, cells were pre-treated with the following inhibitors: Pertussis Toxin (PTX, 200 ng/ml, 2h, 37 °C followed by washing and re-equilibration in serum free, TNF-α containing medium for 2h), C3 transferase (C3, 3.75 μg/ml, 2h at 37 °C), PP2 (10 μM, 30 min at 37 °C), LY294002 (LY, 10 μM, 30 min at 37 °C), prior to CD47 crosslinking for the indicated times. With the exception of PTX, inhibitors were maintained in the medium during antibody crosslinking of CD47.

Immunofluorescence microscopy

Confluent ECs in 35 mm dishes were cultured in serum-free medium overnight in the presence of TNF-α (10 ng/ml). CD47 crosslinking was performed by addition of anti-CD47

primary mAb for 30 min, followed by goat anti-mouse AlexaFluo488 Ab (Invitrogen) for the indicated time points. Cells were then fixed in 3.7% formaldehyde and permeabilized in PBS-0.1% Triton x-100. F-actin was detected by phalloidin-Alexa Fluo594 (Invitrogen) and VEC was detected by anti-VEC polyclonal Ab (sc-6458, Santa Cruz) followed by donkey-anti goat AlexaFluo647 Ab (Invitrogen). Fluorescent clusters dimensions were measured with ImageJ software. Briefly, serial confocal sections were stacked, a relative threshold was applied and images were binarized. CD47 clusters were counted and data were expressed as relative area. At least three separated experiments were quantified. In experiments designed to investigate the formation of transmigratory cups, human $CD4^+$ T cells were allowed to migrate for 30 min on human lung microvascular ECs previously transfected with human CD47-GFP, before fixing the samples in 3.7% formaldehyde and staining with Cholera Toxin Texas Red (Invitrogen) to visualize T cells. To investigate molecule colocalization, anti-ICAM1 coated beads were allowed to adhere for 20 min on TNF-α stimulated human lung microvascular ECs before fixation and staining with biotinylated anti-CD47 mAb (5 μg/ml), followed by Alexa Fluor 488- streptavidin (Invitrogen), and in house conjugated anti-ICAM1-AlexaFluo594 and anti-VCAM1-AlexaFluo617. Molecule co-localization was determined by Pearson's Analysis using LSM Image software.

Live cell imaging and analysis

Live cell imaging was performed on an Axiovert S200 microscope equipped with an Orca CCD camera (Hamamatsu), Axiovision software (Zeiss) using a 40x (1.3 n.a.) oil immersion objective[3]. Confluent GPNT or primary rat endothelial cells in Delta-T live cell imaging dishes (Bioptechs) were serum starved overnight in the presence of TNF-α (10 ng/ml). For calcium imaging, cells were loaded with Fura-2 AM (2 μM, Molecular Probes) in HBSS for 30 minutes at 37 °C. Cells were washed twice in serum free medium and stimulated either with anti-CD47 mAb (10 μg/ml), anti-ICAM1 mAb (10 μg/ml), anti-MHC Class I (10 μg/ml) or IgG1 isotype control mAb (10 μg/ml) followed by cross-linking with goat-anti mouse mAb (10 μg/ml). Ionomycin (2 μM) was added at the end as loading control. Where indicated, cells were pre-treated with BAPTA-2AM (20 μg/ml, 30 min at 37 °C) or PP2 (10 μg/ml, 60 min at 37 °C). Ratiometric calcium flux was calculated (340_{nm}EX:510_{nm}EM-background/380_{nm}EX:510_{nm}EM-background) for each cell[4].

Immunoprecipitation and western blotting

Immunoprecipitation, SDS-PAGE and western blotting were performed as previously reported[1]. Briefly, TNF stimulated confluent rat endothelial monolayers were left untreated or pre-treated with the indicated inhibitors, prior to lysis in boiling 50 mM Tris/Cl, pH 6.8, 2% SDS, 10% glycerol, 100 mM DTT, 100 nM calyculin A (200 μl/60-mm dish). The p-AKT and p-src were detected by anti-phospho-AKT (Ser473) and an anti-phospho-src (Tyr416) Abs (Cell Signaling). Total src and AKT were detected by AKT Ab (9272) and src Ab (2108) from Cell Signaling. For VEC immunoprecipitation cells were washed in HBSS containing 1 mM vanadate and lysed in RIPA buffer (50 mM Tris, 150 mM NaCl containing 0.2% SDS, 1% Triton-x100, 1% Sodium Deoxycholate, 5 mM EDTA, 1 mM orthovanadate and protease inhibitors (Sigma-Aldrich, St Louis, MO, USA). Clarified cell extracts were incubated with 3 μg of anti-VEC Ab (sc-6458, Santa Cruz) and antigen-antibody complexes were collected by protein G-sepharose beads (Sigma-Aldrich, St Louis, MO, USA). For

detection of VEC phospho-tyrosine658 and 731, confluent rat MVEC were pre-treated and stimulated as detailed in figure legends, and then lysed in the above buffer, and SDS-PAGE and western blotting were performed as described previously[1,5]. Specific anti-VEC Abs (product # 441145G and 441144G) were purchased from Life Technologies. Total VEC was determined with sc6458 Ab (Santa Cruz). Quantitation of VEC phosphorylation by western blot was determined as follows. The intensity of the protein band signals were quantitated using Image J. The values for the phosphoprotein intensities were normalized to the total VEC loading, and the ratio of the values of crosslinked versus uncrosslinked for each treatment were calculated as the fold-change in phosphorylation due to crosslinking of CD47.

Preparation of Ab-coated beads

Polystyrene beads (10 μm in diameter, Bangs Laboratories) were incubated with 50 μg/ml purified anti-ICAM1 mAb (R6.5) at room temperature with rocking for 18 h. BSA at a final concentration of 1 mg/ml was then added and the mixture was incubated for an additional 2 h followed by washing six times in PBS. Beads were either used immediately or stored at 4°C for several days before use.

EC Permeability Assay

GPNT cells were plated onto collagen-coated Costar transwells (0.4-μm pore size, 6.5-mm diameter polycarbonate filters). Confluent GPNT were serum starved over night prior to performing the experiment. To measure permeability, medium in the upper chamber was replaced with HBSS without phenol red containing fluorescein-labeled dextran (FITC-dextran, 0.5 mg/ml, 70 kDa, anionic; Invitrogen). After 1h to allow for equilibration, 50μl of medium was collected from the bottom well and then replaced with 50μl of fresh serum free medium at intervals of 15 min for 90 min, before addition of thrombin (1U/ml) or anti-CD47 mAb (clone OX101, 10μg/ml) for 10 min followed by secondary goat anti-mouse Ab (GAM, 10μg/ml). Measurements were carried out every 15 min for a total of 4h. Medium collected from the bottom chamber was the analysed for fluorescence using a fluorescent plate reader (CytoFluor II, PerSeptive Biosystems). Data are shown at 60 min post primary antibody addition. Each assay was performed in triplicate.

T cells

Myelin basic protein (MBP)-specific rat T cell lines were prepared as described[1]. Splenic rat T cells were purified from 6–8 weeks old female Lewis rats by positive selection using $CD4^+$ MACS beads (Miltenyi, Auburn, CA, USA) per manufacturer's instructions. T cells were cultured in anti-CD3 mAb coated plates, soluble mAb CD28 and recombinant IL-2 for 72h and expanded with IL-2 (25 U/ml). Human whole blood was processed using Ficoll Paque to collect mononuclear leukocytes and CD4+ T cells were isolated by positive selection using $CD4^+$ MACS beads and cultured in the presence of human recombinant IL-2 (50 U/ml). Blood was drawn and handled according to protocols for protection of human subjects approved by the Brigham and Women's Hospital Institutional Review Board. Informed consent was obtained from all volunteers in accordance with the Declaration of Helsinki. Rat and human T cells were cultured in RPMI-1640 supplemented with 10% FCS,

100 U/ml penicillin, 100 μg/ml streptomycin, 1 mM sodium pyruvate, 1 mM nonessential amino acids, 2 mM L-Gluamine, and 50 μm β-mercaptoethanol.

Lymphocyte Adhesion

For adhesion assays, rat T cells were fluorescently labeled with 1 μM 2′,7′-bi-(2-carboxyethyl)-5-(and-6)- carboxyfluorescein, acetoxymethyl ester (BCECF, AM, Molecular Probes) for 30 min at 37°C before addition to EC monolayers (approximately ten labeled T cells per EC). Co-cultures were left at 37°C for 15 minutes and adherent T cells quantified in a fluorescent plate reader at excitation/emission wavelengths of 485/520 nm. Wells without T cells were used to assay the background fluorescence. Unbound T cells were aspirated and wells were washed with pre warmed HBSS four times, 100 μl HBSS was added to each well and plates were scanned to assay a number of bound cells. The percentage of bound cells was calculated as a ratio between the fluorescence of washed and unwashed wells after subtraction of the background fluorescence. Results are expressed as percentage of control adhesion. At least three independent experiments were conducted for each treatment.

Lymphocyte Transmigration

Confluent GPNT cells were activated overnight with TNF-α (10 ng/ml) before use. Where indicated, ECs were pre-incubated with either anti-CD47 mAb (30 μg/ml), anti-ICAM1 mAb (30 μg/ml) or anti-IgG1 isotype control mAb (30 μg/ml) for 30 min and T cells were added and allowed to migrate under static conditions for 2h or under flow. Samples were fixed and stained for CD4 (Alexa-594 conjugated or Cholera Toxin-Alexa 594) or CD47 and VEC followed by secondary rabbit-anti mouse Alexa-488 conjugated and donkey anti-rabbit Alexa-647 conjugated. Transmigration was quantified by confocal microscopy.

Statistical Analysis

Data are presented as mean ± SEM. Variances of mean values were analyzed by the Student's *t* test. *$p < 0.05$; **$0.001 < p < 0.01$; ***$p \leq 0.001$. Time-course data were analyzed by linear regression, and the significance of slopes was determined by analyses of covariance (ANCOVA) (Prism software package).

Supplementary Material

Refer to Web version on PubMed Central for supplementary material.

Acknowledgments

Sources of funding:

NIH grants to FWL (HL36028 and HL53993) and CVC (HL104006), and by support from the Wellcome Trust and the Rosetrees Trust (JG, RM).

Abbreviations/acronyms

TEM	transendothelial cell migration
PI3K	phosphoinositide3-kinase

EC	endothelial cell
VEC	Vascular Endothelial Cadherin
MVEC	microvascular endothelial cell
GAM	goat anti-mouse
ICAM-1	intercellular adhesion molecule-1
VCAM-1	vascular adhesion molecule-1
MHC	Major histocompatibility complex

References

1. Barreiro O, Martin P, Gonzalez-Amaro R, Sanchez-Madrid F. Molecular cues guiding inflammatory responses. Cardiovasc Res. 2010; 86:174–182. [PubMed: 20053659]
2. Barreiro O, Yanez-Mo M, Serrador JM, Montoya MC, Vicente-Manzanares M, Tejedor R, Furthmayr H, Sanchez-Madrid F. Dynamic interaction of VCAM-1 and ICAM-1 with moesin and ezrin in a novel endothelial docking structure for adherent leukocytes. J Cell Biol. 2002; 157:1233–1245. [PubMed: 12082081]
3. Carman CV, Jun CD, Salas A, Springer TA. Endothelial cells proactively form microvilli-like membrane projections upon intercellular adhesion molecule 1 engagement of leukocyte LFA-1. J Immunol. 2003; 171:6135–6144. [PubMed: 14634129]
4. Carman CV, Springer TA. A transmigratory cup in leukocyte diapedesis both through individual vascular endothelial cells and between them. J Cell Biol. 2004; 167:377–388. [PubMed: 15504916]
5. Alcaide P, Auerbach S, Luscinskas FW. Neutrophil recruitment under shear flow: it's all about endothelial cell rings and gaps. Microcirculation. 2009; 16:43–57. [PubMed: 18720226]
6. Weber C, Fraemohs L, Dejana E. The role of junctional adhesion molecules in vascular inflammation. Nat Rev Immunol. 2007; 7:467–477. [PubMed: 17525755]
7. Liao F, Ali J, Greene T, Muller WA. Soluble domain 1 of platelet-endothelial cell adhesion molecule (PECAM) is sufficient to block transendothelial migration in vitro and in vivo. J Exp Med. 1997; 185:1349–1357. [PubMed: 9104821]
8. Turowski P, Adamson P, Greenwood J. Pharmacological targeting of ICAM-1 signaling in brain endothelial cells: potential for treating neuroinflammation. Cell Mol Neurobiol. 2005; 25:153–170. [PubMed: 15962512]
9. Brown EJ, Frazier WA. Integrin-associated protein (CD47) and its ligands. Trends Cell Biol. 2001; 11:130–135. [PubMed: 11306274]
10. Lindberg FP, Bullard DC, Caver TE, Gresham HD, Beaudet AL, Brown EJ. Decreased resistance to bacterial infection and granulocyte defects in IAP-deficient mice. Science. 1996; 274:795–798. [PubMed: 8864123]
11. Su X, Johansen M, Looney MR, Brown EJ, Matthay MA. CD47 deficiency protects mice from lipopolysaccharide-induced acute lung injury and Escherichia coli pneumonia. J Immunol. 2008; 180:6947–6953. [PubMed: 18453616]
12. Fortin G, Raymond M, Van VQ, Rubio M, Gautier P, Sarfati M, Franchimont D. A role for CD47 in the development of experimental colitis mediated by SIRPalpha+C. J Exp Med. 2009; 206:1995–2011. [PubMed: 19703989]
13. Lamy L, Foussat A, Brown EJ, Bornstein P, Ticchioni M, Bernard A. Interactions between CD47 and thrombospondin reduce inflammation. J Immunol. 2007; 178:5930–5939. [PubMed: 17442977]
14. Azcutia V, Stefanidakis M, Tsuboi N, Mayadas T, Croce KJ, Fukuda D, Aikawa M, Newton G, Luscinskas FW. Endothelial CD47 promotes vascular endothelial-cadherin tyrosine

phosphorylation and participates in T cell recruitment at sites of inflammation in vivo. J Immunol. 2012; 189:2553–2562. [PubMed: 22815286]

15. de Vries HE, Hendriks JJ, Honing H, De Lavalette CR, van der Pol SM, Hooijberg E, Dijkstra CD, van den Berg TK. Signal-regulatory protein alpha-CD47 interactions are required for the transmigration of monocytes across cerebral endothelium. J Immunol. 2002; 168:5832–5839. [PubMed: 12023387]
16. Liu Y, Merlin D, Burst SL, Pochet M, Madara JL, Parkos CA. The role of CD47 in neutrophil transmigration. Increased rate of migration correlates with increased cell surface expression of CD47. J Biol Chem. 2001; 276:40156–40166. [PubMed: 11479293]
17. Rosseau S, Selhorst J, Wiechmann K, Leissner K, Maus U, Mayer K, Grimminger F, Seeger W, Lohmeyer J. Monocyte migration through the alveolar epithelial barrier: adhesion molecule mechanisms and impact of chemokines. J Immunol. 2000; 164:427–435. [PubMed: 10605039]
18. Stefanidakis M, Newton G, Lee WY, Parkos CA, Luscinskas FW. Endothelial CD47 interaction with SIRPgamma is required for human T-cell transendothelial migration under shear flow conditions in vitro. Blood. 2008; 112:1280–1289. [PubMed: 18524990]
19. Johansen ML, Brown EJ. Dual regulation of SIRPalpha phosphorylation by integrins and CD47. J Biol Chem. 2007; 282:24219–24230. [PubMed: 17584740]
20. Yang L, Kowalski JR, Yacono P, Bajmoczi M, Shaw SK, Froio RM, Golan DE, Thomas SM, Luscinskas FW. Endothelial cell cortactin coordinates intercellular adhesion molecule-1 clustering and actin cytoskeleton remodeling during polymorphonuclear leukocyte adhesion and transmigration. J Immunol. 2006; 177:6440–6449. [PubMed: 17056576]
21. Turowski P, Martinelli R, Crawford R, Wateridge D, Papageorgiou AP, Lampugnani MG, Gamp AC, Vestweber D, Adamson P, Dejana E, Greenwood J. Phosphorylation of vascular endothelial cadherin controls lymphocyte emigration. J Cell Sci. 2008; 121:29–37. [PubMed: 18096689]
22. Martinelli R, Gegg M, Longbottom R, Adamson P, Turowski P, Greenwood J. ICAM-1-mediated endothelial nitric oxide synthase activation via calcium and AMP-activated protein kinase is required for transendothelial lymphocyte migration. Mol Biol Cell. 2009; 20:995–1005. [PubMed: 19073885]
23. Brown DA, London E. Structure and function of sphingolipid- and cholesterol-rich membrane rafts. J Biol Chem. 2000; 275:17221–17224. [PubMed: 10770957]
24. Huang AJ, Manning JE, Bandak TM, Ratau MC, Hanser KR, Silverstein SC. Endothelial cell cytosolic free calcium regulates neutrophil migration across monolayers of endothelial cells. J Cell Biol. 1993; 120:1371–1380. [PubMed: 8449983]
25. Su WH, Chen HI, Huang JP, Jen CJ. Endothelial [Ca(2+)](i) signaling during transmigration of polymorphonuclear leukocytes. Blood. 2000; 96:3816–3822. [PubMed: 11090065]
26. Isenberg JS, Roberts DD, Frazier WA. CD47: a new target in cardiovascular therapy. Arterioscler Thromb Vasc Biol. 2008; 28:615–621. [PubMed: 18187671]
27. Allingham MJ, van Buul JD, Burridge K. ICAM-1-mediated, Src- and Pyk2-dependent vascular endothelial cadherin tyrosine phosphorylation is required for leukocyte transendothelial migration. J Immunol. 2007; 179:4053–4064. [PubMed: 17785844]
28. Alcaide P, Newton G, Auerbach S, Sehrawat S, Mayadas TN, Golan DE, Yacono P, Vincent P, Kowalczyk A, Luscinskas FW. p120-Catenin regulates leukocyte transmigration through an effect on VE-cadherin phosphorylation. Blood. 2008; 112:2770–2779. [PubMed: 18641366]
29. Carman CV, Sage PT, Sciuto TE, de la Fuente MA, Geha RS, Ochs HD, Dvorak HF, Dvorak AM, Springer TA. Transcellular diapedesis is initiated by invasive podosomes. Immunity. 2007; 26:784–797. [PubMed: 17570692]
30. Rebres RA, Green JM, Reinhold MI, Ticchioni M, Brown EJ. Membrane raft association of CD47 is necessary for actin polymerization and protein kinase C theta translocation in its synergistic activation of T cells. J Biol Chem. 2001; 276:7672–7680. [PubMed: 11114301]
31. Alcaide P, Martinelli R, Newton G, Williams MR, Adam A, Vincent PA, Luscinskas FW. p120-Catenin prevents neutrophil transmigration independently of RhoA inhibition by impairing Src dependent VE-cadherin phosphorylation. Am J Physiol Cell Physiol. 2012; 303:C385–C395. [PubMed: 22648953]

32. Adamson P, Wilbourn B, Etienne-Manneville S, Calder V, Beraud E, Milligan G, Couraud PO, Greenwood J. Lymphocyte trafficking through the blood-brain barrier is dependent on endothelial cell heterotrimeric G-protein signaling. FASEB J. 2002; 16:1185–1194. [PubMed: 12153986]

33. Adamson P, Etienne S, Couraud PO, Calder V, Greenwood J. Lymphocyte migration through brain endothelial cell monolayers involves signaling through endothelial ICAM-1 via a rho-dependent pathway. J Immunol. 1999; 162:2964–2973. [PubMed: 10072547]

34. Zhou M, Brown EJ. Leukocyte response integrin and integrin-associated protein act as a signal transduction unit in generation of a phagocyte respiratory burst. J Exp Med. 1993; 178:1165–1174. [PubMed: 8104228]

35. Greenwood J, Wang Y, Calder VL. Lymphocyte adhesion and transendothelial migration in the central nervous system: the role of LFA-1, ICAM-1, VLA-4 and VCAM-1 off. Immunology. 1995; 86:408–415. [PubMed: 8550078]

36. Sumagin R, Lomakina E, Sarelius IH. Leukocyte-endothelial cell interactions are linked to vascular permeability via ICAM-1-mediated signaling. Am J Physiol Heart Circ Physiol. 2008; 295:H969–H977. [PubMed: 18641276]

References

1. Martinelli R, Gegg M, Longbottom R, Adamson P, Turowski P, Greenwood J. ICAM-1-mediated endothelial nitric oxide synthase activation via calcium and AMP-activated protein kinase is required for transendothelial lymphocyte migration. Mol Biol Cell. 2009; 20:995–1005. [PubMed: 19073885]

2. Yang L, Froio RM, Sciuto TE, Dvorak AM, Alon R, Luscinskas FW. ICAM-1 regulates neutrophil adhesion and transcellular migration of TNF-alpha-activated vascular endothelium under flow. Blood. 2005; 106:584–592. [PubMed: 15811956]

3. Martinelli R, Kamei M, Sage PT, Massol R, Varghese L, Sciuto T, Toporsian M, Dvorak AM, Kirchhausen T, Springer TA, Carman CV. Release of cellular tension signals self-restorative ventral lamellipodia to heal barrier micro-wounds. J Cell Biol. 2013; 201:449–465. [PubMed: 23629967]

4. Sage PT, Varghese LM, Martinelli R, Sciuto TE, Kamei M, Dvorak AM, Springer TA, Sharpe AH, Carman CV. Antigen recognition is facilitated by invadosome-like protrusions formed by memory/effector T cells. J Immunol. 2012; 188:3686–3699. [PubMed: 22442443]

5. Stefanidakis M, Newton G, Lee WY, Parkos CA, Luscinskas FW. Endothelial CD47 interaction with SIRPgamma is required for human T-cell transendothelial migration under shear flow conditions in vitro. Blood. 2008; 112:1280–1289. [PubMed: 18524990]

Significance

We provide evidence that endothelial CD47 engagement activates intracellular signaling pathways known to be involved in TEM and include mobilization of intracellular calcium, increased permeability, and activation of the src and AKT/PI3K in primary isolated rat brain microvascular endothelial cells and in a rat brain endothelial cell line. These signaling pathways also elicited cytoskeleton remodeling and VEC tyrosine phosphorylation, which have been demonstrated as necessary events during T cell TEM. We also demonstrate that during T cell migration, transmigratory cups and podoprints enriched in CD47 are detected in endothelium, indicating that spatial redistribution of CD47 occurs following its engagement. This information implicates CD47 as an important molecule in T cell transendothelial migration.

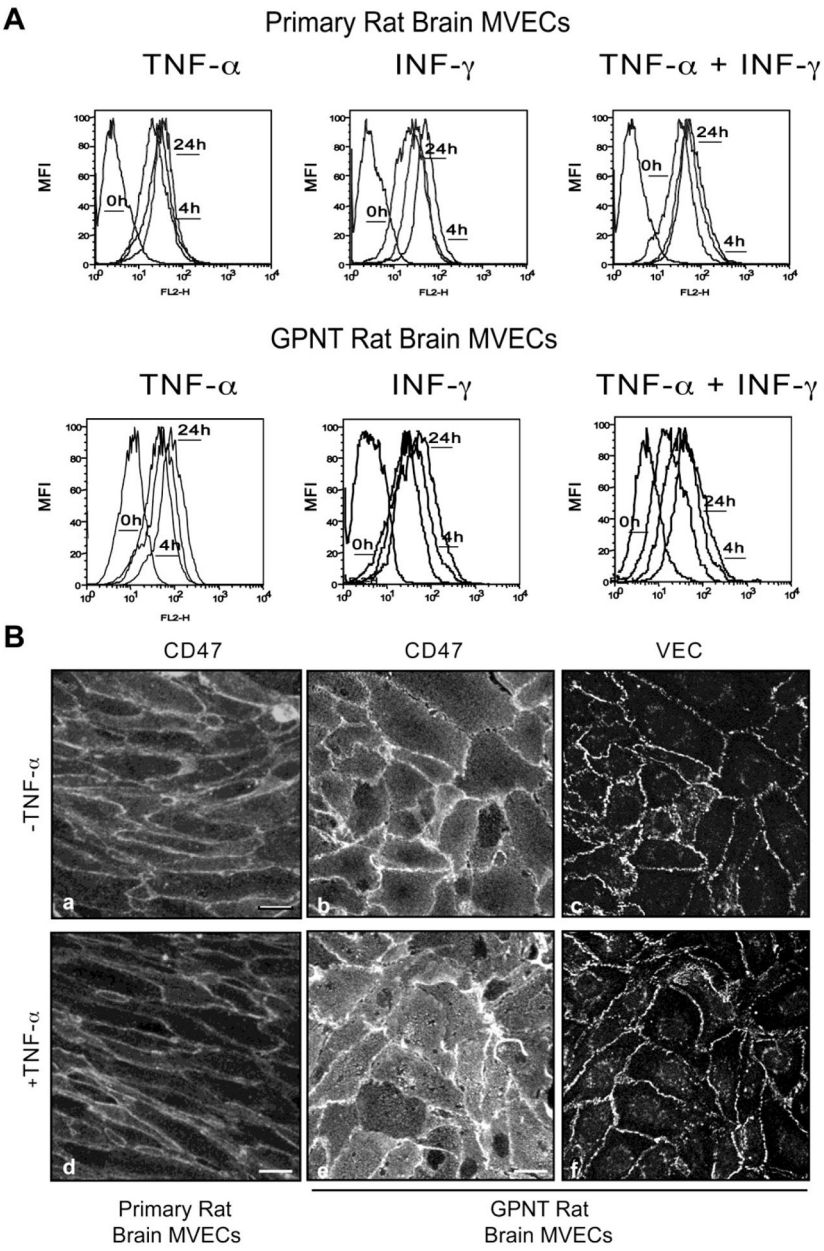

Figure 1. Cell Surface Expression and Localization of CD47 in rat brain MVEC

(A) Primary rat brain MVEC and the rat brain cell line GPNT (lower panel) were either left untreated or treated with TNF-α (10 ng/mL), IFN-γ (100 U/mL), or both for 4h or 24h. CD47 expression was quantified by flow cytometry using anti-CD47 mAb and an isotype-match non-binding control mAb. (B) Primary rat brain MVEC (a, d) and GPNT (b, c, e, f) cells were left untreated or treated with TNF-α for 24h, fixed and stained for CD47 and VEC. Data are representative of three experiments. Bars=10 μm.

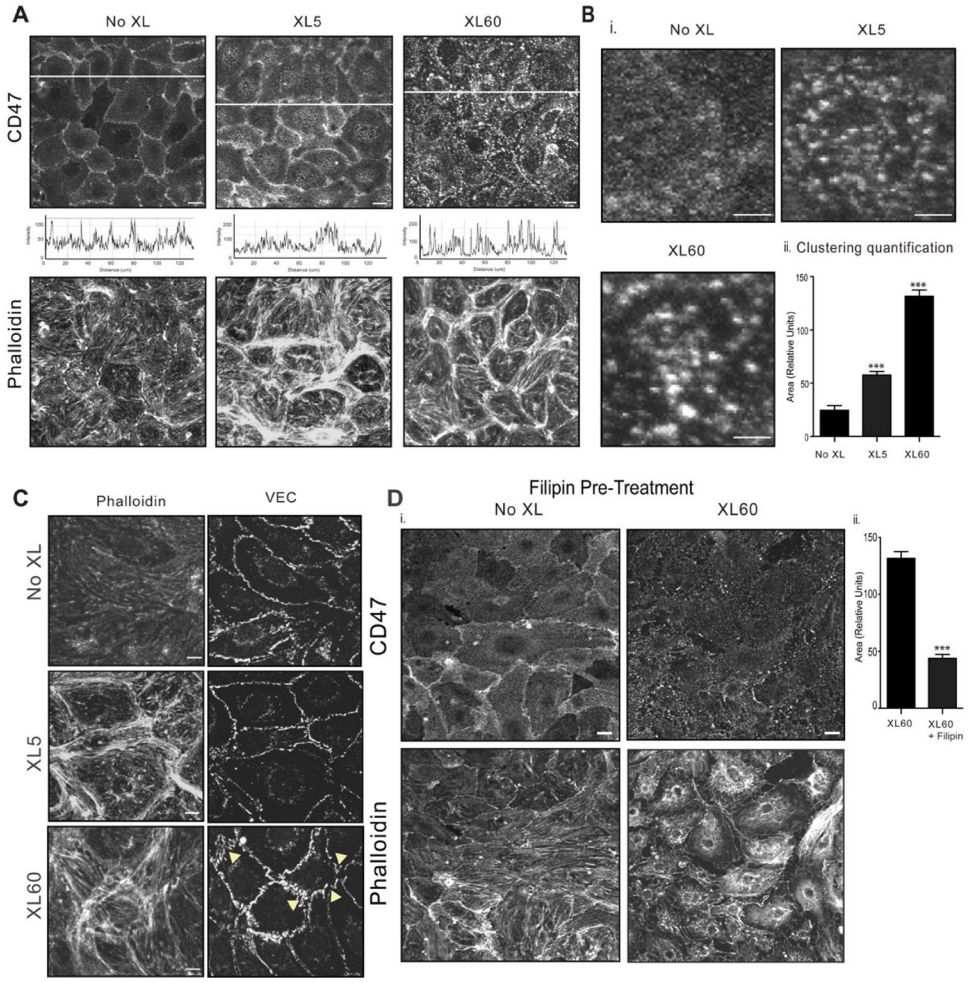

Figure 2. Engagement of endothelial CD47 results in receptor clustering and actin rearrangements

(A) CD47 and actin (phalloidin) staining in confluent TNF-α stimulated GPNT cells after crosslinking primary anti-CD47 mAb with goat-anti mouse polyclonal Ab (GAM) for the indicated times. The fluorescence intensity of CD47 as assessed using quantitative image analysis of fluorescence (x–y plots below panel a–c). B). CD47 cluster dimension was calculated as described in Methods. Bar=2 μm. (C) As in A, phalloidin staining of F-actin or VEC. Bar=5 μm. Data are representative of three or more separate experiments. (D) Confluent serum starved, TNF-α stimulated GPNT were treated with filipin (10 μg/ml, 30 min at 37 °C) before CD47 crosslinking for 60 min. CD47 and F-actin are shown. The cluster dimension was measured as described in Methods. Data are mean ± SEM, n=3. Bar=10 μm.

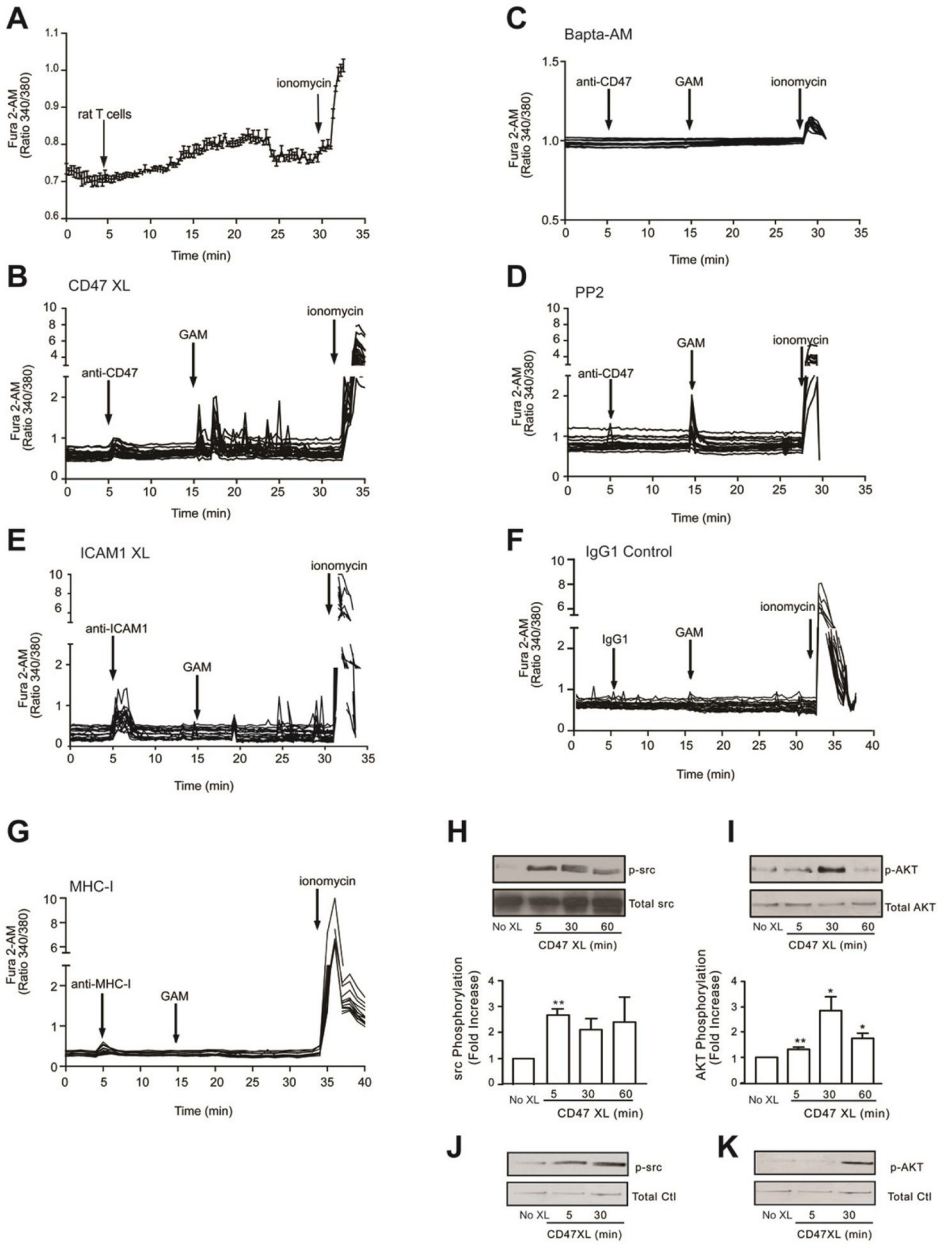

Figure 3. CD47 induces calcium release, src and AKT phosphorylation in rat brain MVEC

(A–G) Confluent serum starved, TNF-α stimulated GPNT were loaded with Fura-2 AM. Intracellular calcium release was monitored by live cell fluorescence microscopy. Where indicated, rat T cells were added or GPNT cells were stimulated with 10 μg/ml of mAb to CD47, ICAM1, MHC-I, GAM, or mouse IgG1 control mAb. Where indicated, cells were pre-treated with BAPTA-2AM (20 μM, 30 min at 37 °C) or PP2 (10 μM, 60 min at 37 °C) prior to CD47 engagement. Data are representative of three experiments. (H–K) CD47 was crosslinked as indicated on confluent, serum starved, TNF-α stimulated GPNT cells. Changes in p-src and p-AKT were quantified by western blot as detailed in Methods. The ratio of the phosphoproteins ÷ total protein were normalized to the control (No XL) to determine fold increase in phosphorylation. Data are means ± SEM, n=3. (J, K) As in H,

except that primary rat brain MVEC were used. Data are representative of two separate experiments.

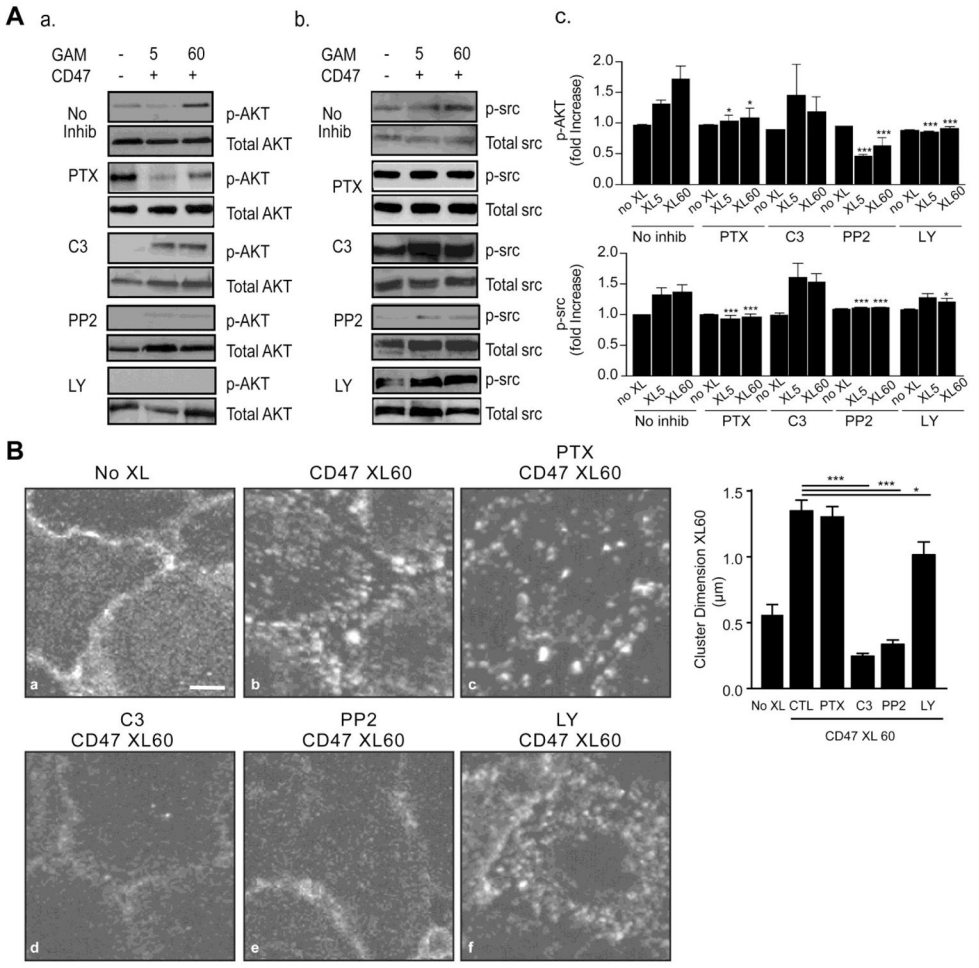

Figure 4. Effect of specific inhibitors on CD47 induced signalling

(A) Confluent serum starved, TNF-α stimulated GPNT cells were left untreated (no XL) or crosslinked with anti-CD47 mAb for 5 or 60 minutes. Where indicated, cells were pre-treated with inhibitors as described in Methods. Cell lysates were probed for p-AKT (a) and p-src (b) as described in Methods. Normalized values obtained by densitometry analysis of bands show the fold increase in absorbance of p-AKT Ser-473 or p-src Tyr416 with respect to total AKT or total src, respectively, for 5 and 60 min XL condition and normalized to the respective non-XL control values (c). (B) Cells treated as in A were fixed and stained for CD47. Images are representative of at least three separate experiments and the graph shows the CD47 cluster dimension analysis. Bar = 5 µm.

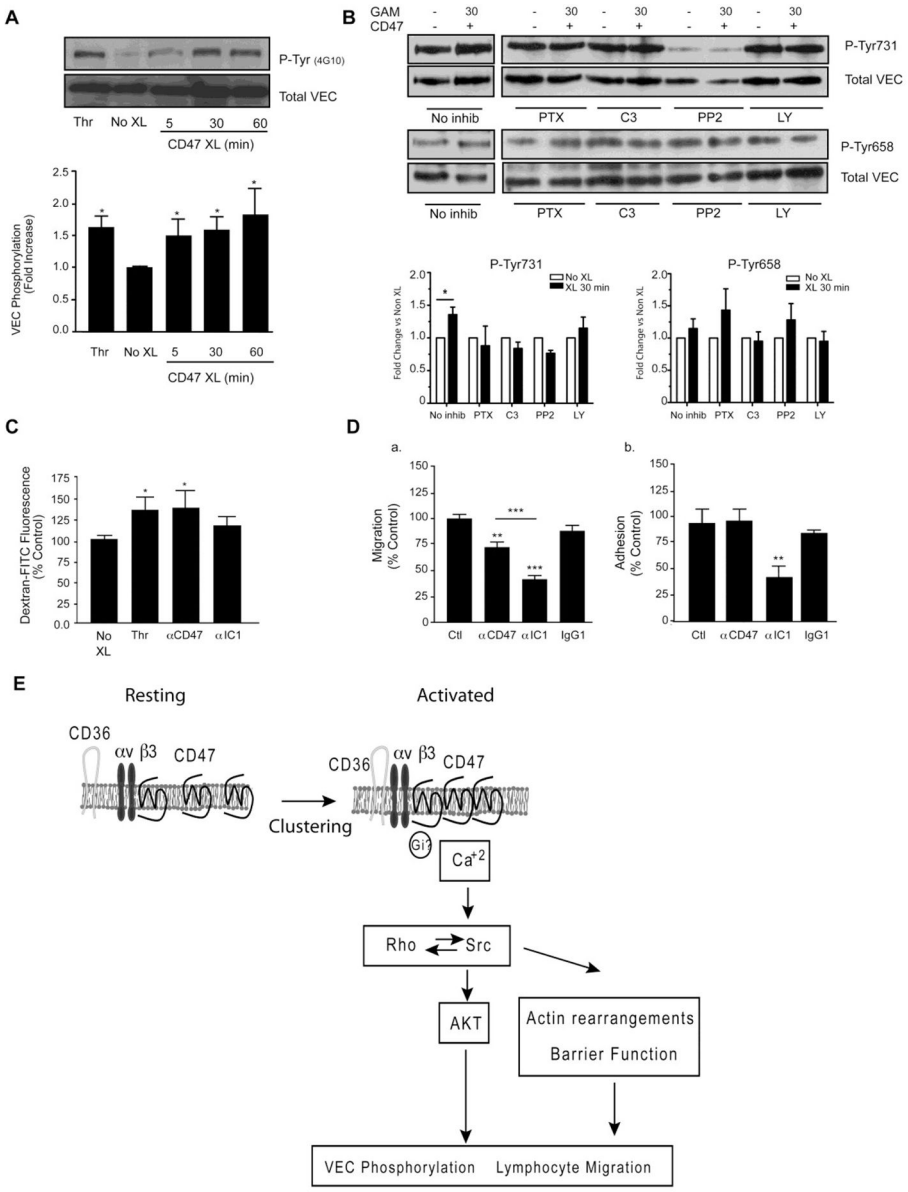

Figure 5. Effect of specific inhibitors on CD47 induced VEC phosphorylation

(A) Confluent serum starved, TNF-α stimulated GPNT cells were left untreated (No XL) or crosslinked with anti-CD47 mAb for the indicated times. Thrombin (Thr, 1 U/ml, 15 min) was used as a positive control. VEC was immunoprecipitated and immunoblotted with the phosphotyrosine specific antibody 4G10 to determine VEC tyrosine phosphorylation. A representative blot and densitometric quantification is shown. Data are mean ± SEM, n=3. Quantification was performed as described in Fig. 3(B) Cells were treated with inhibitors prior to performing CD47 crosslinking for 30 min. Phospho-Tyr658 and 731 VEC were detected by immunoblot analysis of lysates as detailed in Methods. A representative blot and densitometric quantification of four experiments are shown (mean±SEM). (C) Permeability to Dextran-FITC was assessed as described in Methods. Results are normalized to untreated control (No XL). (D) Transmigration (a) and adhesion (b) of rat T cells under flow was

performed as described in Methods. Results are mean ± SEM of duplicates from three independent experiments. (E) Schematic representation of intracellular signalling pathways induced by CD47 engagement in the endothelium. See discussion for additional detail.

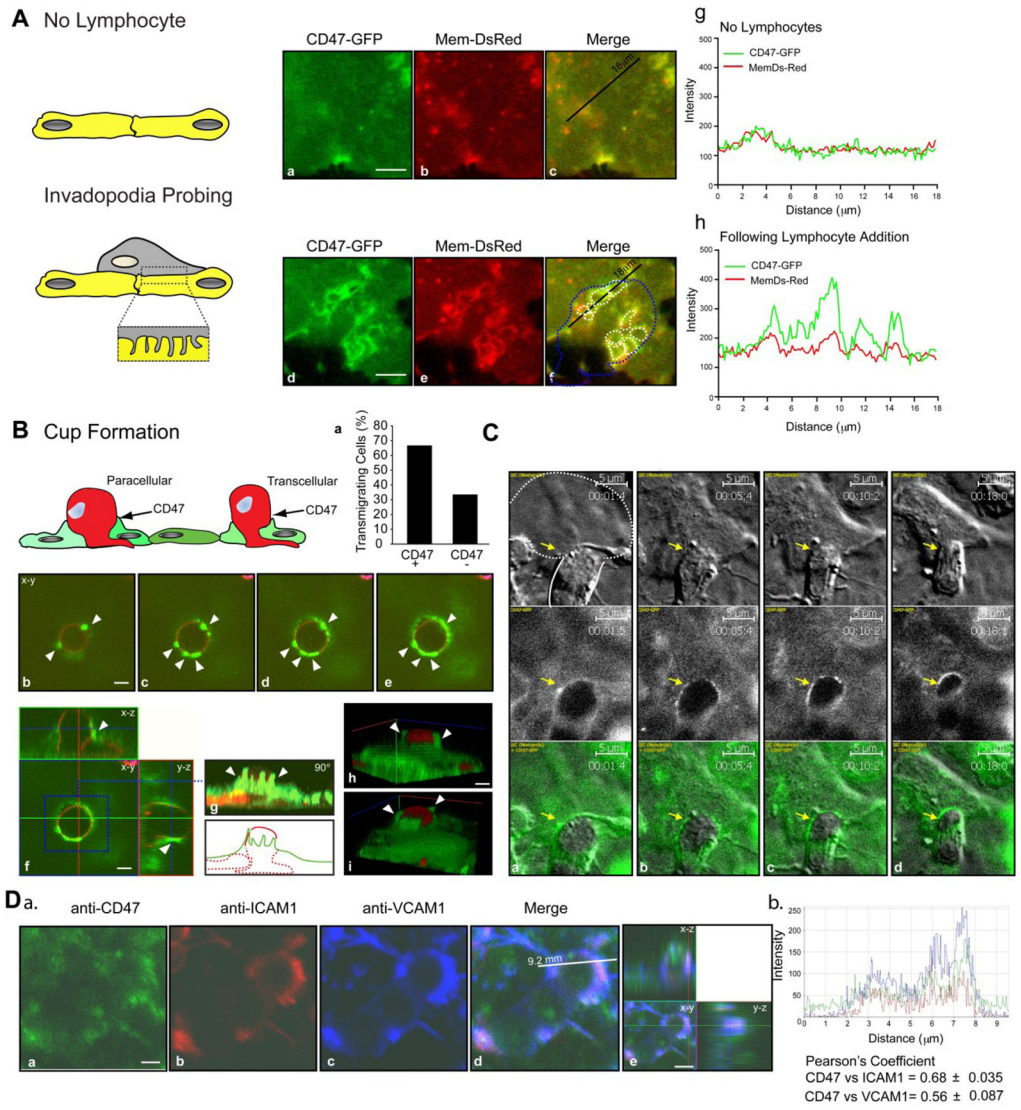

Figure 6. Endothelial CD47 is enriched at the site on T cell transcellular migration

(A) Human T cells were allowed to migrate on HLMVECs expressing human CD47-GFP and Mem-DsRed. Panels a–c show CD47-GFP and Mem-DsRed distribution in a subcellular region. Panels d–f show the same region following podoprint (white dashed lines) induced by the T cell (contour shown in dashed blue line in panel f). Panels g–h are representative line scan (see black line in c and f) analyses that show the relative fluorescence intensity of Mem-DsRed and CD47-GFP. Note that in the absence of podoprints (panels a–c), both markers show similar intensity profiles, whereas CD47 is significantly enriched relative to Mem-DsRed within podoprints (panels d–f). Bar = 5μm. (B) T cell transmigration is associated with endothelial CD47 projections. MBP-activated rat T cells were allowed to migrate for 15 min on rat MVECs, followed by fixation and staining T cells with Cholera Toxin-B subunit-AlexaFluor-546 (a GM1 ganglioside probe that identifies T cells) and with anti-CD47 mAb followed by Alexa Fluo 488 anti-mouse secondary Ab. The graph (panel a) shows the quantification of CD47 enrichment in transmigrating T cells. Confocal serial

section images are shown in panels a–d. The orthogonal projection in panel f shows the transmigrating T cell being enveloped by CD47 enriched projections. Panels h and i show 3D rendering of confocal serial sections processed with the Axiovision Software. The white arrows indicate sites of CD47 enrichment on the endothelium. Bar = 5μm. 3D rendering corresponding to (B) is provided as supplemental video S1. (C) Live-cell imaging of human T cell migration on HLMVECs transiently transfected with human CD47-GFP. The white line represents the T cell (dotted, under the endothelium; continuous, above the endothelium). The arrow heads show sites of CD47 enrichment. Bar = 5μm. *Time lapse videos corresponding to (C) are provided as* supplemental video S2. (D) a. Anti-ICAM1 mAb coated beads were allowed to adhere on TNF-α stimulated HLMVECs for 20 min before fixation and staining for CD47, ICAM1 and VCAM1. Shown is a representative image with correspondent orthogonal view (a–e). Bar = 2.5μm. b. Representative linescan (see white line in e) analysis for CD47, ICAM1 and VCAM1 co-localization.